

# Structural and optical properties of $\text{CuIn}_{1-x}\text{Ga}_x\text{Se}_2$ thin films

N. M. A HADIA, M. M. WAKKAD\*, E. KH. SHOKR, Y. TAYA  
*Physics Department, Faculty of Science, Sohag University, Sohag, Egypt*

Bulk alloys of  $\text{CuIn}_{1-x}\text{Ga}_x\text{Se}_2$  with Ga – incorporation ratio  $x = \text{Ga} / (\text{Ga} + \text{In})$  equal to 0.1, 0.2, 0.3, 0.4 and 0.6 have been prepared by the melt quench technique. The  $\text{CuIn}_{1-x}\text{Ga}_x\text{Se}_2$  (CIGS) thin films have been deposited on clean microscope glass substrates with different thickness (50, 100, 150, 200 and 250 nm) using the thermally evaporated technique in a vacuum of  $3 \times 10^{-4}$  mbar from the prepared bulk material. XRD, SEM and EDAX were utilized in order to examine the structure, surface morphology and composition stoichiometry of CIGS samples. Effects of Ga – ratio, film thickness and annealing at 573 K for different periods of time (5 – 60 min.) on structural and optical properties have been depicted and explained. Some important structural and optical parameters were calculated and discussed.

(Received April 26, 2018; accepted February 17, 2020)

*Keywords:* Cu  $\text{In}_{1-x}\text{Ga}_x\text{Se}_2$  (CIGS), Bulk alloys, thin films, Annealing, Structural investigations, XRD, Optical properties

## 1. Introduction

Now all the world research for clean energy sources concerns new sources such as wind, waterfalls, geothermal and solar energy. Great attention has been paid to the solar cells with high efficiency and low cost. Currently, Nanjing South Railway Station planning to implement slate roof renovation is integrating solar cell modules into traditional roof materials to generate clean energy [1].

Many compounds can be used to fabricate the solar cells, and they are classified into many generations. One of the preferred compounds in this field is the quaternary  $\text{CuIn}_{1-x}\text{Ga}_x\text{Se}_2$  (CIGS) compound. The excellent absorption characteristics of this polycrystalline chalcopyrite structure in the form of thin film recommend it to be an attractive candidate for use as an absorber material for photovoltaic applications [2-5], and regarded as a promising candidate for thin film solar cell modules [6]. This CIGS compounds have a high potential for solar energy conversion because of their direct band gap and high absorption coefficient [6–8].

Several methods of deposition techniques have been used to prepare CIGS films [9], such as physical vapor deposition (PVD) technique [6], co evaporation [10, 11], sputtering techniques [12], spray pyrolysis [13], electron-beam evaporation [14], and other methods such as selenization of metallic precursors [15-17], and thermal evaporation technique have been used to prepare CIGS film with suitable physical and environmental properties needed for higher efficiency solar cell absorbing layer.

Efficiency exceeding 20% has been reported for solar cells based on CIGS [4, 18, and 19]. To our knowledge, the maximum energy conversion efficiency, up to now, has reached 22.6% on a co – evaporated

Cu (In, Ga)  $\text{Se}_2$  small area [20]. Further progress in CIGS cell efficiency toward 25% could be expected by improving further the optical and the electrical efficiencies

[21]. Number of experimental results [2, 22-24] emphasizes that the substitution of In in  $\text{CuInSe}_2$  thin films by small amounts of the isovalent Ga not only increases the open circuit voltage  $V_{OC}$  of the solar cell and raises the band gap to more suitably match AM1.5 solar spectrum, but may also improve the electrical properties of CIGS films. Therefore, the progress in cell efficiency requires deep investigation and optimization of the central parameters of all cell parts that determine the design and performance of a solar cell. The present work focuses on CIGS absorber layer because of its significant importance in solar cell technology.

The main parameters of semiconducting CIGS solar cell absorber layer that determine its performance are the microstructure parameters such as the degree and orientation of film crystallinity, grain size, dislocation density and/or concentration of doping atoms, which affect on carriers transport, their generation and recombination processes and/ or the width of space charge region of a junction. In addition, the band gap  $E_g$ , the absorption coefficient ( $\alpha$ ), the refractive index ( $n$ ) characterizing the ability of a semiconducting material to absorb visible and other radiation as well as the extinction coefficient ( $k$ ) that describes the rate of radiation attenuation along the propagation direction are considered as fundamental parameters need to be used in solar cell applications [25].

Thus, the investigation of the experimental tools and the data of such parameters may allow for understanding of the sequential growth process of CIGS thin films and identification of the associated changes in their optoelectronic properties. Moreover, CIGS absorber thin film of more than  $1\mu\text{m}$  thick has been usually utilized in order to increase its light absorption. Nevertheless, it is believed that, thinner CIGS layer of around 250 – 300 nm, receiving less attention, may be sufficient to absorb the useful part of spectrum due to its high absorption

coefficient ( $10^5 \text{ cm}^{-1}$ ) in addition to its greatly reducing the material usage and associated cost.

Therefore, this article aims to study the structure and optical properties of  $\text{CuIn}_{1-x}\text{Ga}_x\text{Se}_2$  thin films synthesized by thermal evaporation technique. Besides, the effects of In – substitution by small amounts of the isovalent Ga in terms of the ratio  $x = \text{Ga} / (\text{Ga} + \text{In}) = 0.1, 0.2, 0.3, 0.4$  and  $0.6$  of Ga- incorporation (Ga – ratio, for brevity), annealing conditions as well as film thickness on micro structural and optical parameters have been considered. Relatively thinner films of  $50 - 250 \text{ nm}$  thick were employed in order to examine their capability as CIGS solar cell absorber layers.

## 2. Experimental methods

Bulk CIGS were prepared by melt quench technique. Elemental constituents of high purity (99.999%) were sealed in an evacuated ( $\sim 10^{-5}$  mbar) quartz ampoule and heated gradually from  $373 \text{ K}$  up to  $1073 \text{ K}$ , for period extended to 16 hrs. as shown in table (1). The thin films of  $\text{CuIn}_{1-x}\text{Ga}_x\text{Se}_2$  with different thicknesses ( $50, 100, 150, 200$  and  $250 \text{ nm}$ ) have been deposited by thermal evaporation of bulk materials using a coating unit (Manufactured using Technology Licensed from Edwards Ltd, Auto 306, 2014).

Table 1. Temperature - time for bulk alloys preparation.

T (K)	373	473	573	673	773	873	973	1073
t ( hrs)	1	1	1	2	2	3	3	3

Thin film samples were annealed at  $573 \text{ K}$  for periods of time of 5, 10, 20, 30, 40 and 60 min using a digital furnace type Lindberg (USA model 51442 combined with a controller unit model 58114). The x-ray diffraction (XRD) examinations have been carried out using x- ray diffractometer type Philips (Holland model PW 1710). The pattern of XRD analysis was run in normal 2 theta scan with Cu as a target and Ni as a filter ( $\lambda = 1.541838 \text{ \AA}$ ) at  $40 \text{ kV}$  and  $30 \text{ mA}$ , with scanning speed  $2^\circ/\text{min}$ . A scanning range of  $2\theta$  from  $4^\circ$  to  $80^\circ$  was used. The crystallite sizes as well as micro strain of the films were estimated using Debye-Scherrer formula [26, 27]. The surface morphology has been examined using Quanta FEG 250 scanning electron microscope (FEI) company, USA. The chemical and stoichiometric composition analysis has been performed using SM model Quanta 250 FEB attached with EDAX unit with acclimation voltage  $30 \text{ KV}$  magnification 14 up to 1000000 and resolution for gun In.

Values of the transmittance (T) and reflectance (R) were measured at room temperature for both the as – deposited and annealed films, using a computer-programmable (Jasco V-570, Japan) double beam spectrophotometer in the wavelength range from  $200-2500 \text{ nm}$  at normal incidence with a scan speed of  $400 \text{ nm}/\text{min}$ . To measure the reflectivity, an additional attachment (model ISN – 470, Japan) is provided. The optical constants definitely, the refractive index (n) and the extinction coefficient (k) of as - deposited and annealed

CIGS thin films were determined using the measured transmittance and reflectance.

## 3. Results and discussion

### 3.1. Microstructure characterization

XRD patterns of the prepared CIGS alloys in bulk and thin film forms presented in Figs. (1and 2) reveal the polycrystalline structure of these considered materials. The predominant peaks in XRD diffractograph of CIGS alloys could be probably associated with (112), (204/220), (116/312) and (316/332) reflections of the chalcopyrite structure [28]; which is in agreement with the international center for diffraction data (ICDD) structure card number (JCPDS 01-079-7081). Besides, secondary phases, such as Se,  $\delta\text{-In}_2\text{Se}_3$ ,  $\text{Cu}_2\text{Se}_x$  and  $\text{CuSe}_2\text{O}_5$  with low intensity could be detected, which indicate a little structure distortion formed in the alloy [28, 29]. The (ICDD) structure card numbers for those secondary phases are (JCPDS 24-1202, 20-049, 47-4448 and 30-0503), respectively.

By comparing XRD diffractograms in Fig.(1a,b), it could be concluded that, the evident reduction in the intensity and even disappearance of some secondary phases, after film synthesizing by thermal deposition from its initial bulk form, indicate a predominance of the single phase chalcopyrite CIGS in film structure. These disappeared secondary phases may be dissolved during deposition and imbedded in the amorphous matrix.

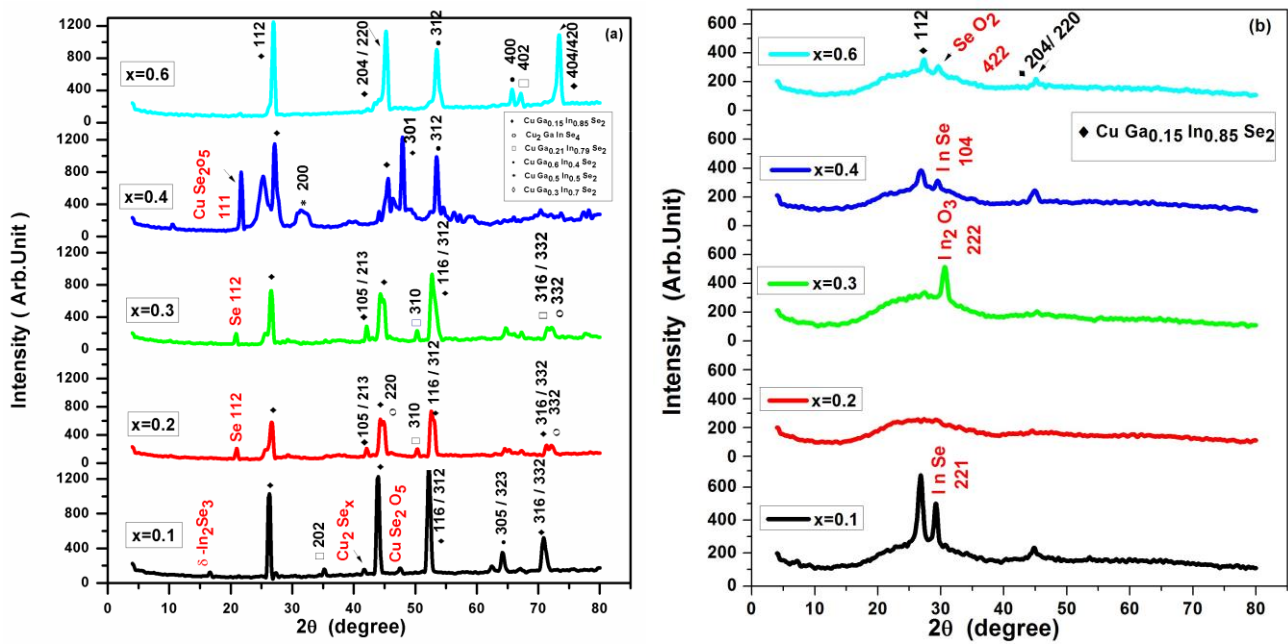


Fig. 1. (a) XRD patterns for bulk and (b) thin film of  $\text{CuIn}_{1-x}\text{Ga}_x\text{Se}_2$  alloys before annealing (color online)

Although XRD patterns confirm the distinct polycrystalline nature of the origin bulk CIGS material, the as deposited films seemed to be partially amorphous, since a hump characterizing the amorphous matrix is clearly seen in the range  $15^\circ \leq 2\theta \leq 40^\circ$ . Excluding the film with  $x = 0.2$ , which seems to be nearly amorphous, the increase of Ga – ratio in films leads to the decrease in the intensities and sharpness of the existed peaks resulting in a decrease of the structure ordering of a film. These bulk and film feature differences may be attributed to the change in micro strain of bulk and film forms and/ or the phase dissociation during thermal deposition, a matter that significantly affected not only on the elements ratio in the considered CIGS compound, but also on the whole material texture.

To extract the effect of annealing process on the CIGS microstructure, thin films of the  $\text{CuIn}_{0.9}\text{Ga}_{0.1}\text{Se}_2$  composition, for example, were considered. The effect of annealing at temperature  $T_a = 573$  K for the periods  $t_a = 5$  and 60 min on these films is displayed as shown in fig. (2). It is shown that, the annealing process doesn't change the main CIGS internal structure, where the most interest peaks of (112) orientation at  $2\theta \approx 26.81^\circ$ , and (204/220) orientation at  $2\theta \approx 44.47^\circ$  still appear. Only, it is observed that the annealing process increases the intensity of the observed intense peaks leading to the enhancement of their crystallinity.

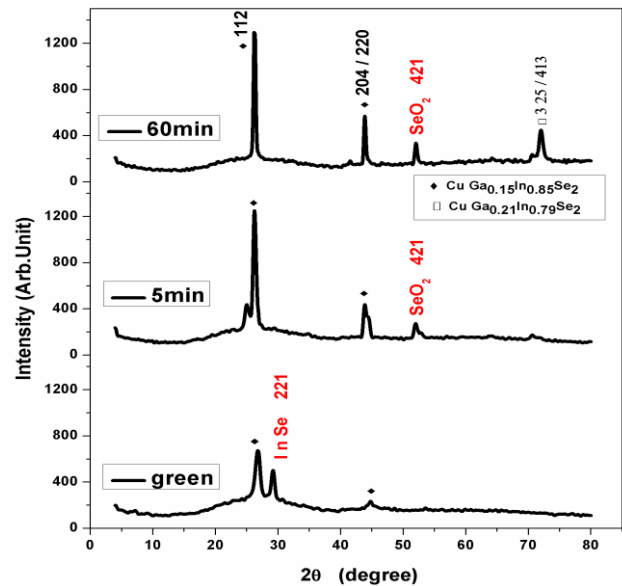


Fig. 2. XRD patterns for as - deposited thin films of  $\text{CuIn}_{0.9}\text{Ga}_{0.1}\text{Se}_2$  alloy and after annealing at 573 K for 5 and 60 min (color final)

The lattice parameters (a, c) and the volume of the unit cell (v) have been calculated for bulk and thin film CIGS samples by using computer program. An example of the extracted data of bulk  $\text{CuIn}_{1-x}\text{Ga}_x\text{Se}_2$  alloys is shown in Fig. (3).

The changes in the lattice parameters ( $a$ ,  $c$ , and  $v$ ) for bulk  $\text{CuIn}_{1-x}\text{Ga}_x\text{Se}_2$  alloys with Ga- ratio, which are:  $a \approx (5.70\text{--}5.88)$  Å,  $c \approx (11.35\text{--}11.6)$  Å and  $v \approx (370\text{--}400)$  Å<sup>3</sup>, are consistent with that recorded for  $\text{CuIn}_{1-x}\text{Ga}_x\text{Se}_2$  by the international center for diffraction data (ICDD). This may confirm the success in preparing tetragonal CIGS alloy by using melt quench method. The observed general decrease in the values of these parameters with increasing Ga- ratio, excluding the values of  $c$  and  $v$  having slight increases at  $x=0.3$  and  $0.6$  which enhances the material compactness, may be expected since the atomic volume of Ga is smaller than that of In.

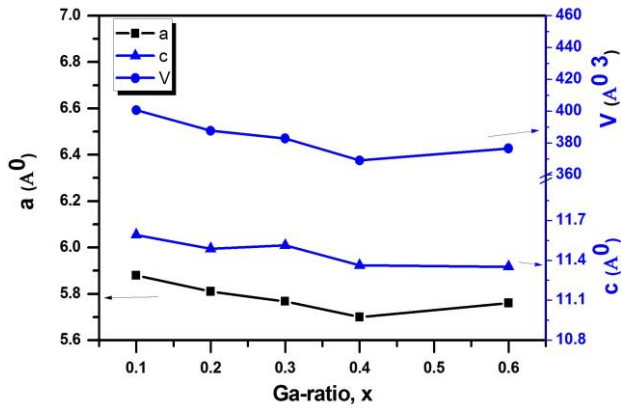


Fig. 3. The lattice parameters  $a$ ,  $c$  and the volume of the unit cell  $v$  for bulk  $\text{CuIn}_{1-x}\text{Ga}_x\text{Se}_2$  (color online)

The crystallite parameters such as the average crystallite size ( $D$ ) [26, 27], the dislocation density ( $\delta$ ) [26, 30 & 31], the number of crystallites per unit area ( $N$ ) and the micro strain ( $\epsilon$ ) [26, 32] can be calculated using the following equations, respectively;

$$D = \frac{0.94 \lambda}{\beta \cos \theta} \quad (\text{nm}) \quad (1)$$

$$\delta = \frac{1}{D^2} \quad (\text{nm}^{-2}) \quad (2)$$

$$N = \frac{d}{D^3} \quad (\text{nm}^{-2}) \quad (3)$$

$$\epsilon = \frac{\beta \cos \theta}{4} \quad (4)$$

where  $\beta$  is the value of the full – width at half maximum (FWHM) of the highest peaks of XRD pattern in radian,  $\lambda$  is the wavelength of XRD radiation ( $\lambda=1.541838$ ),  $\theta$  is the Bragg's diffraction angle of the peak and  $d$  is the film thickness. These crystallite parameters have been calculated for bulk and thin film  $\text{CuIn}_{1-x}\text{Ga}_x\text{Se}_2$  alloys and depicted in Fig. 4 and Table 2. It is shown that, the crystallite size decreases with increasing the Ga- ratio from  $x=0.1$  to  $x=0.3$ , then it increases with increasing  $x$  up to  $0.6$ . Inverse views of this behavior are shown for both  $\delta$  and  $\epsilon$ . Data in the range of relatively smaller Ga ratios ( $x=0.1 - 0.3$ ) agree with the results in Fig. 3 and may be explained in terms of the atomic volume difference of Ga and In too. However, the observed increase in crystallite size as well as the decrease in dislocation density with further increases of  $x$  up to  $0.6$  might be related to the extension of the unit cell in this range of  $x$ . Besides, the variations of both  $\delta$  and  $\epsilon$  with Ga- ratio can be accepted regarding the equations (1, 2 and 4) suggesting that  $\epsilon$  and  $\delta$  are inversely proportional to  $D$  and  $D^2$  respectively.

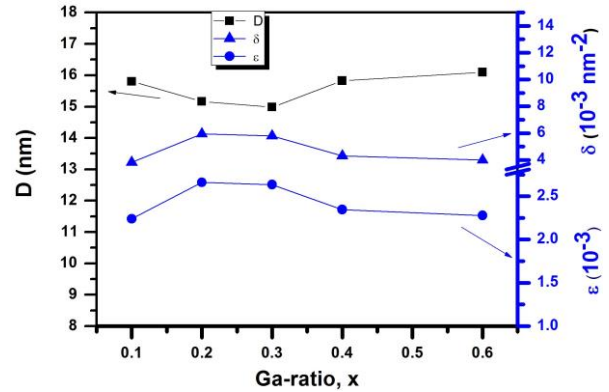


Fig. 4. The dependences of crystallite size ( $D$ ), the dislocation density ( $\delta$ ) and the strain ( $\epsilon$ ) on the Ga –ratio of  $\text{CuIn}_{1-x}\text{Ga}_x\text{Se}_2$  bulk alloys (color online)

Table 2 gives an example for the variations of crystallite size ( $D$ ), the number of crystallites  $N$ , the lattice strain ( $\epsilon$ ) and the dislocation density  $\delta$  with the annealing time  $t_a$  at 573 K for  $\text{CuIn}_{0.9}\text{Ga}_{0.1}\text{Se}_2$  thin films. It is clear that, the elongation of  $t_a$  leads to increase the crystallite size  $D$ , but inhibits the other structural parameters viz  $N$ ,  $\epsilon$  and  $\delta$  as it is predicted by equations (1- 4).

Table 2. The variations of crystallite size ( $D$ ), the number of crystallites  $N$ , the lattice strain ( $\epsilon$ ) and the dislocation density  $\delta$  with the annealing time  $t_a$  at 573 K for  $\text{CuIn}_{0.9}\text{Ga}_{0.1}\text{Se}_2$  thin films

	$a$ (Å)	$c$ (Å)	$v$ (Å <sup>3</sup> )	$D$ (nm)	$\delta$ (nm <sup>-2</sup> )	$\epsilon$	$N$ (nm <sup>-2</sup> )
as- deposited	5.85599	11.2034	384.195	10.50537	0.00912	0.003456197	0.218362743
5 min	5.96546	11.42929	406.730	11.57361386	0.009100901	0.003349023	0.236056523
60 min	6.01565	11.34313	410.485	21.20972	0.00227	0.0017204	0.027328642

In order to investigate the influence of Ga- ratio on the surface morphology of CIGS films, SEM images of as – deposited 250 nm thick CIGS thin films of different values of Ga- ratio ( $x = 0.1, 0.2, 0.3$  &  $0.6$ ) depicted in Fig. (5a, b, c, & d) respectively, have been employed. It is clear that, the as – deposited film of  $x = 0.1$  exhibits some large non – uniform distributed agglomerates on the surface (Fig. 5a), which may correspond to CIGS (112) and / or InSe (221) phases revealed by XRD (Fig 1b), creating a rugged film surface. SEM image for as – deposited film having  $x = 0.2$  confirms its nearly amorphous structure (Fig. 5b). The observed very little grains may be correlated to the tiny (112) and (204 / 220) CIGS phases revealed by XRD (Fig 1b). With increasing Ga –ratio to the value 0.3 or 0.6, slight improvement in film crystallinity could be achieved (Fig. 5 c& d). Little number density of relatively large grains with dark parts, which are imbedded in the

amorphous matrix, could be observed. It is believed that, these dark parts of the CIGS grains may be caused by Se loss [33].

Annealing for 60 min. at 573 K leads to non – identical and more number density of grains on the film surface, Fig 5e. Besides, larger dark grain parts could be observed indicating that Selenium could volatilize and / or might form other compounds like the binary  $\text{SeO}_2$  phase detected by XRD (Fig.2). Furthermore, SEM image shows that, the structure of this annealed film is not entirely crystalline. It still contains a large amorphous matrix. At the end, all the present CIGS films did not show dense, uniform and smooth surface, confirming that the good surface morphology of a film could not be achieved. These results permit to suggest that, in order to improve CIGS surface morphology, further efficient heat treatment is strongly recommended.

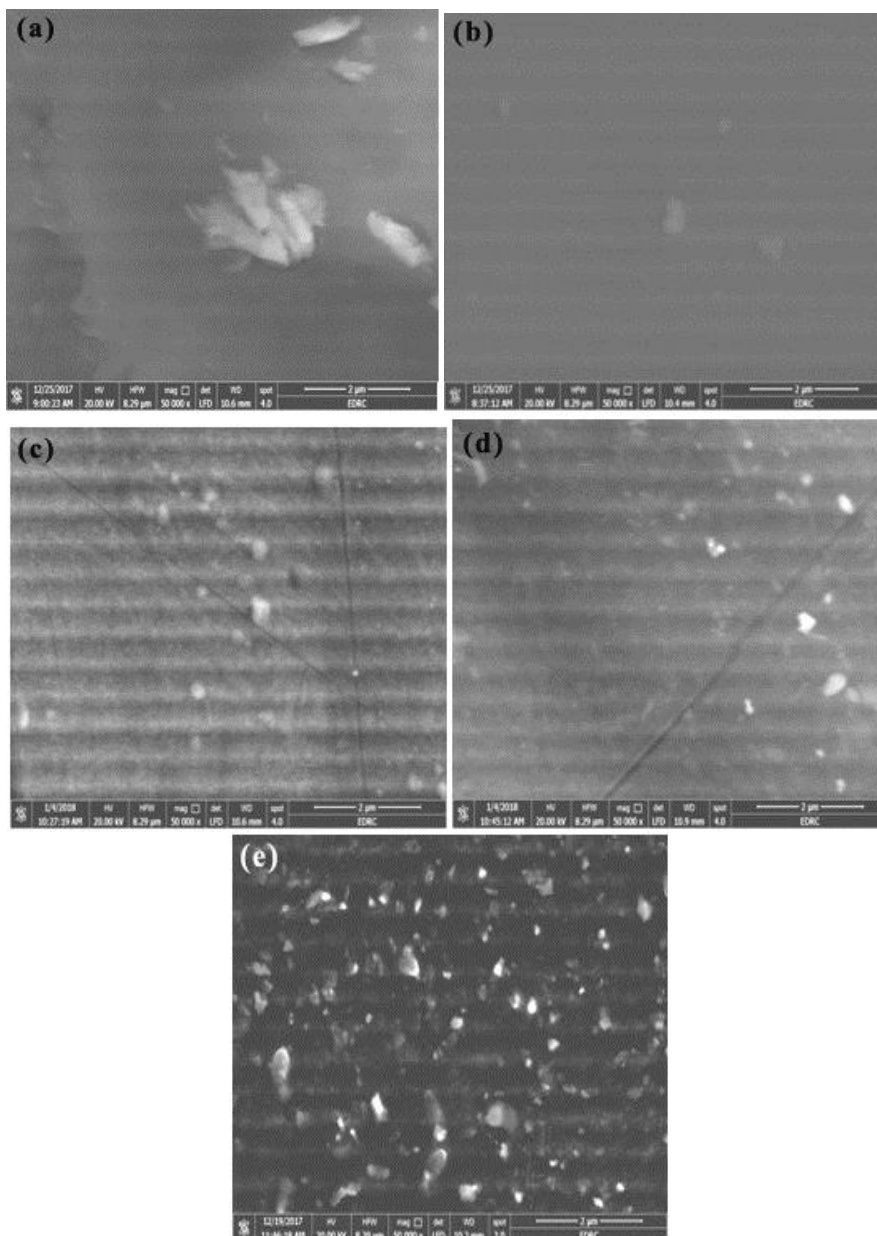


Fig. 5. SEM images for CIGS thin films of 250 nm thick synthesized at different conditions: as – deposited with  $x$  equals to (a) 0.1, (b) 0.2, (c) 0.3, (d) 0.6 and annealed for 60 min. at 573 K with  $x = 0.1$  films

The chemical analysis of the present CIGS films synthesized at different conditions was performed by the EDAX shown in Fig. 6. Data of this figure allow drawing the following conclusions:

(i) No elements, except Cu, In, Ga, Se & O were detected. Ratios of the elemental constituents existed in a film are recorded in Table 3.

Table 3. Ratios of elemental constituents of as – deposited  $\text{CuIn}_{(1-x)}\text{Ga}_{0.x}\text{Se}_2$  with  $x = 0.1$  and  $0.3$  and annealed at 573 K for 60 min. with  $x = 0.1$  thin films; (Thickness = 250 nm)

Ratios of:	Cu	In	Ga	Se	O
X = 0.1 (as – deposit.)	21.45	24.55	1.98	40.60	11.42
X = 0.3 (as – deposit.)	11.26	25.63	8.88	45.33	8.89
X = 0.1 (anneal.)	14.84	15.55	1.30	26.14	42.17

(ii) Individual grains show Cu – deficient and In – rich, indicating that the elemental constituents of compositions seem to be inaccurate controlled. Stoichiometries of elements are (0.81:1:1.53), (0.33:1:1.31) and (0.88:1:1.55) for as – deposited with  $x = 0.1$  &  $0.3$  and annealed at 573 K for 60 min. with  $x = 0.1$  films respectively. Except the as – deposited film with  $x = 0.3$  showing evident deviation of the composition stoichiometry due to Cu deficiency, other films seemed to have near stoichiometric compositions.

(iii) Values of the Ga / (In + Ga) ratio are 0.07, 0.26 and 0.08 while values of Cu / (In + Ga) ratio 0.81, 0.33 & 0.88 for as – deposited ( $x = 0.1$  &  $0.3$ ) and annealed ( $x =$

0.1) films respectively. Otherwise, the reported optimal Ga / (In + Ga) ratio of CIGS absorber for high efficiency CIGS solar cell is considered to be  $\sim 0.3$  [22, 24& 34] and the maximum performance of CIGS thin film solar cell (efficiency = 19.5% and  $E_g = 1.14$  eV) was attained [35,36] when;  $0.88 < \text{Cu} / (\text{In} + \text{Ga}) < 0.95$  and  $\text{Ga} / (\text{In} + \text{Ga}) \approx 0.3$ .

Although the values of the ratios  $\text{Ga} / (\text{In} + \text{Ga}) = 0.26$  and  $\text{Cu} / (\text{In} + \text{Ga}) = 0.88$ , obtained for as – deposited with  $x = 0.3$  and annealed with  $x = 0.1$  films respectively, are close to their reported optimal values, they are not concurrent with each other because they are related to two different films.

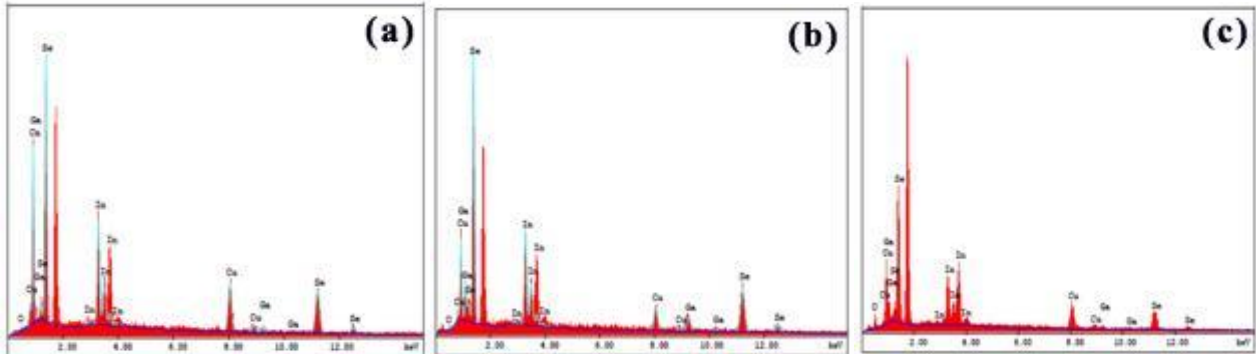


Fig. 6. EDS patterns of CIGS thin films of 250 nm thick. (a) as – deposited,  $x = 0.1$  (b) as – deposited,  $x = 0.3$  and (c) annealed at 573 K for 60 min.,  $x = 0.1$  thin films (color online)

### 3.2. Optical properties

Transmission T and reflection R spectra in the spectral range 200-2500 nm for as – deposited  $\text{CuIn}_{1-x}\text{Ga}_x\text{Se}_2$  thin films processed with different values of Ga – ratios are shown in Fig. 7a, b, respectively. It is clear, that films have absorption edges around solar maximum wavelength ( $\lambda = 500$  nm) with maximum transmission almost in the range 700- 1000 nm of  $\lambda$ . Besides, except the film of  $x = 0.2$  having a relatively higher transmission ( $>70\%$ ) and a shift in the absorption edge towards the

small energies, the transmission of all other films is evidently poor. Furthermore, in NIR region where  $\lambda > 1000$  nm, the reflection of films having very poor transmission ( $< 20\%$ ), is significantly enhanced up to 75%. This effect may be attributed to the plasma oscillations of free carriers pointing out the existence of relatively higher free carriers concentration in these films. Finally, the very good thickness uniformity of the present films may be demonstrated, since interference patterns on the spectra of most films are clearly observed.

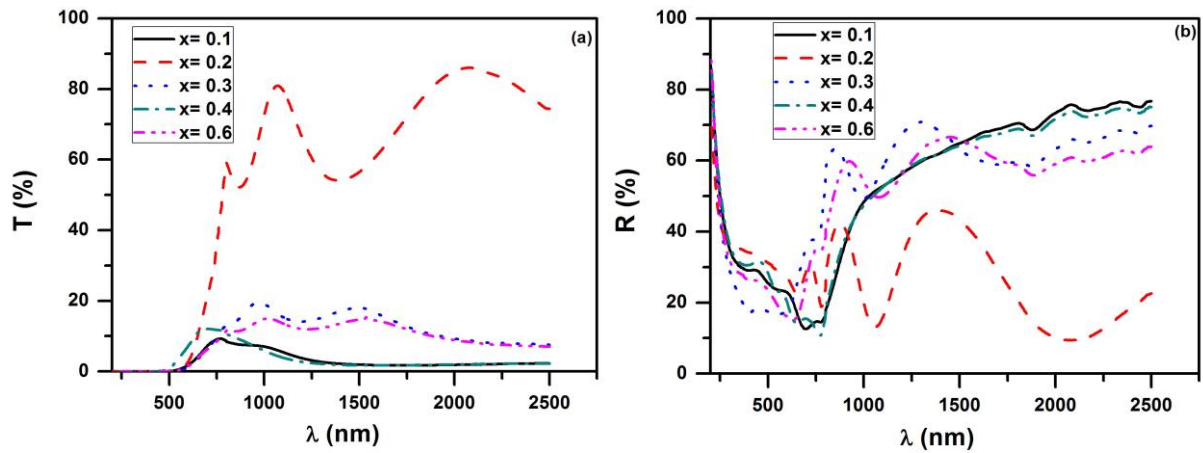


Fig. 7. (a) The dependence of transmittance and (b) the reflectivity on the wavelength of the incident spectrum  $\lambda$  for as – deposited  $\text{CuIn}_{1-x}\text{Ga}_x\text{Se}_2$  thin films with thickness=250 nm (color online)

Fig. 8a, b shows respectively the transmission and reflection spectra of as- deposited  $\text{CuIn}_{0.9}\text{Ga}_{0.1}\text{Se}_2$  films (as an example) with different thicknesses ranging from 50 – 250 nm. Regarding this figure, the following conclusions can be drawn: (i) while the fundamental edge for thinner film (50 nm thick) appeared at  $\lambda \approx 300$  nm, showing the relatively high value of its band gap energy, it appeared at almost the unique value  $\lambda = 500$  nm for the other films. (ii) Excluding the as – deposited thinner film with  $d=50$  nm, for which the transmission increases with increasing  $\lambda$  up

to 2500 nm, the transmission of other films seemed to decrease in NIR spectral region as  $\lambda$  increases, indicating a promotion of excess carrier generation within this region. (iii) The observed transmission peak values of most films within the range  $\sim 700 - 1500$  nm mean that the absorption has started within this range. Finally, all these conclusions could be depicted by using the reflection spectra (Fig. 8b), since the transmission and reflection spectra of the samples has the inverse trend of each other.

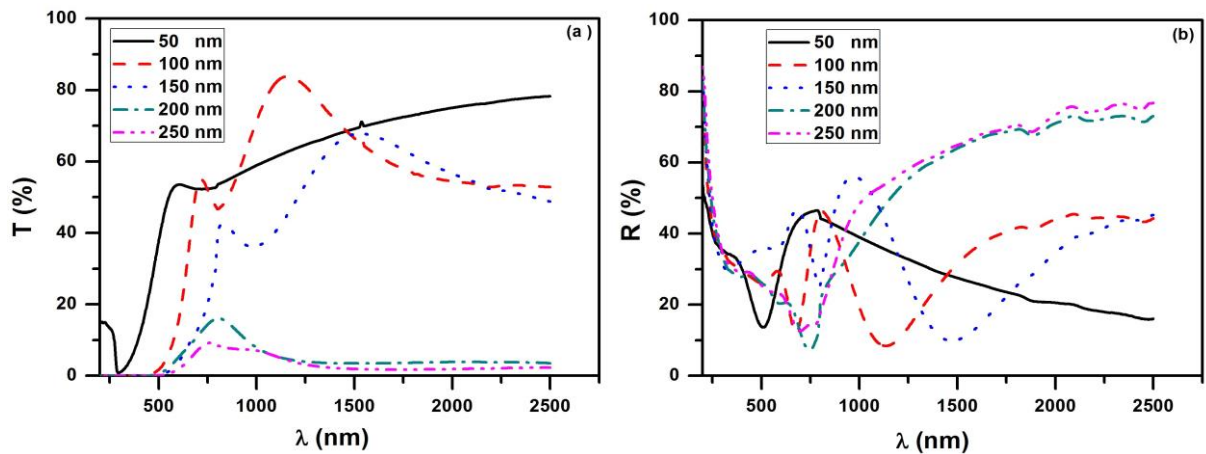


Fig. 8. (a) Transmission and (b) reflection spectra of as – deposited  $\text{CuIn}_{0.9}\text{Ga}_{0.1}\text{Se}_2$  films with different thicknesses (color online)

Annealing process is one of the most factors that can strongly influence on the properties of thin film [9]. In agreement with this concept, the annealing of the present CIGS films is associated with significant effects on both T and R spectra as it is shown in Fig. 9. The maximum transmission value increases from  $\sim 9$  % for as – deposited film to be in the range of 25 -30 % for annealed films at 573 K for different (5-60 min.) periods. Significant effect

of annealing in terms of reflection spectrum inhabitation is observed too. Shifts of the fundamental absorption edge to higher energy values could be deduced for all annealed films with respect to that of the as – deposited one. This may suggest an increase of the energy gap width due to annealing. These observations could be attributed to the crystallinity increase in film micro structure caused by annealing.

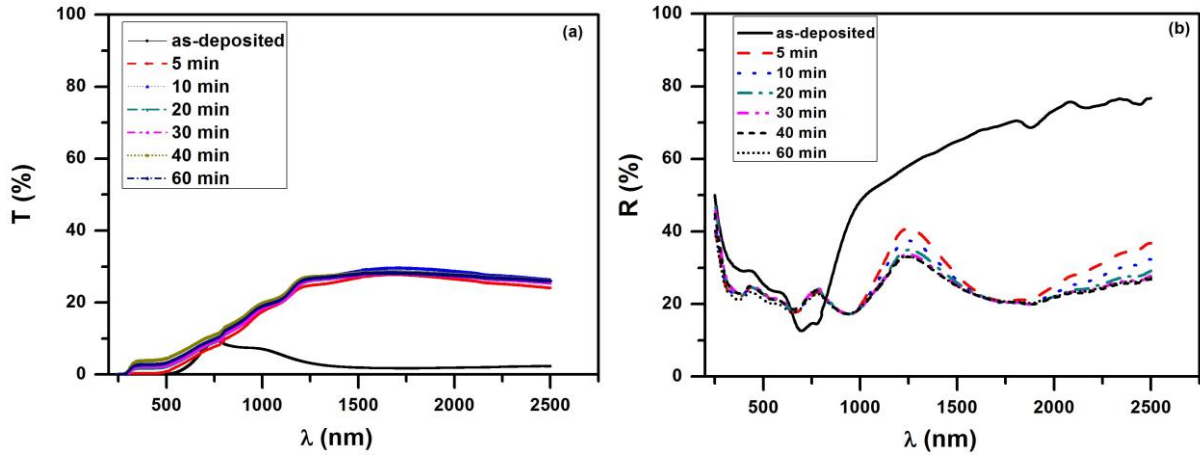


Fig. 9. (a) The dependences of transmittance and (b) the reflectivity with  $\lambda$  for as - deposited and annealed at 573 K (for different periods of time)  $\text{CuIn}_{0.9}\text{Ga}_{0.1}\text{Se}_2$  thin films (film thickness  $\sim 250$  nm) (color online)

In order to calculate the optical parameters of CIGS films, namely, the absorption coefficient ( $\alpha$ ), the refractive index ( $n$ ) and the extinction coefficient ( $k$ ), transmission and reflection spectra such as that presented in Figs. (7, 8 & 9) were utilized through the following equations [37, 38-40]:

$$\alpha = \frac{2.303}{d} \log \left[ \frac{(1-R)^2}{T} \right] \quad (5)$$

$$n = \frac{1+R}{1-R} \pm \left[ \left( \frac{1+R}{1-R} \right)^2 - (1+k^2) \right]^{\frac{1}{2}} \quad (6)$$

$$k = \frac{\alpha \lambda}{4\pi} \quad (7)$$

where  $d$  is the film thickness.

The influences of both composition and thickness on the absorption coefficient of as - deposited films are shown in Fig. (10 a & b). The high values of the absorption coefficient ( $\sim 10^5 \text{ cm}^{-1}$ ) recorded, in general, for the present relatively thinner films of 50-250 nm thick, may confirm the capability of CIGS thinner films for solar cell absorber layer. Besides, the absorption coefficient seemed to be inhibited as Ga- ratio increased. This may be demonstrated by other authors [33], who observed absorption decrease as Ga- ratio exceeds 0.3 and explained it by the larger band gap due to the crystallinity increase with Ga- ratio. Otherwise, the absorption coefficient seemed to be enhanced with increasing film thickness especially at higher values of  $\lambda$ . Thicker films were seen more opaque relative to the thinner ones. This result is believed to be attributed to the increase of free carrier's absorption in this  $\lambda$  - range.

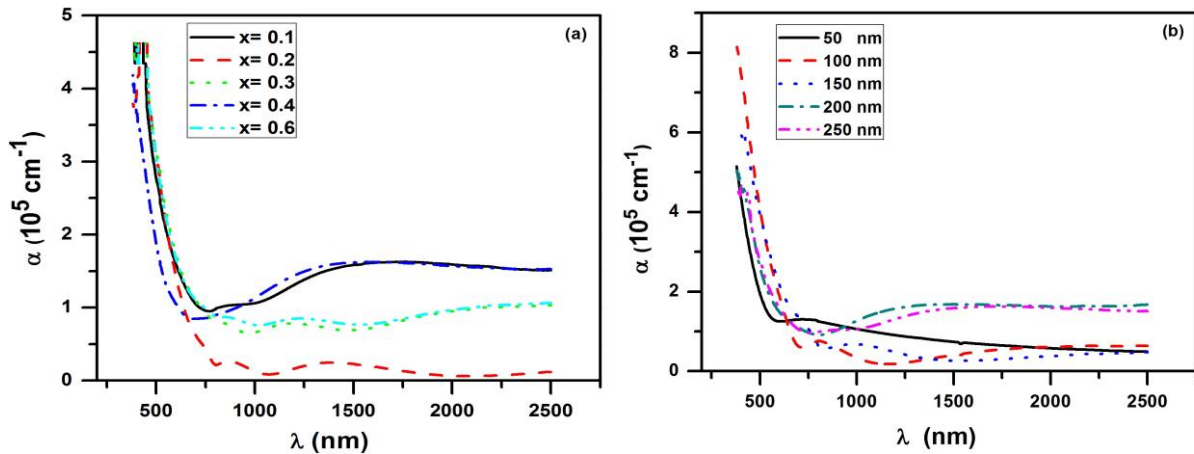


Fig. 10. (a) The absorption coefficient  $\alpha$  versus  $\lambda$  for as - deposited  $\text{CuIn}_{1-x}\text{Ga}_x\text{Se}_2$  thin films with different Ga ratios and (b) for different thicknesses of as - deposited  $\text{CuIn}_{0.9}\text{Ga}_{0.1}\text{Se}_2$  films (color online)

Fig. 11 shows the effects of both Ga- ratio and the film thickness on the variation of  $n$  with  $\lambda$  of the incident spectrum. The present data emphasize the pronounced effects of chemical composition and film thickness on the

measured refractive index. The change in the  $n$  values of a film can be ascribed to the change in its internal microstructure. On the other hand, the characteristic peaks of the refractive index in the lower wavelength region

( $\lambda < 1500$  nm) can be explained using multi oscillator model [40, 41]. The anomalous dispersion of refractive index spectra may be due to the resonance effect between

the incident electromagnetic radiation and the electrons polarization, which leads to the coupling of electrons in CIGS films to the oscillating electric field [42, 43].

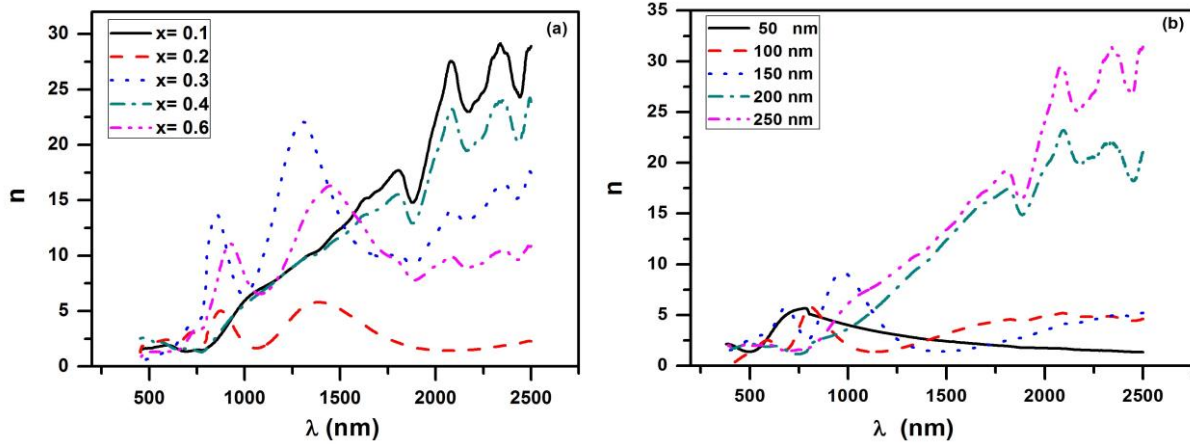


Fig. 11. (a) The refractive index  $n$  versus  $\lambda$  for as – deposited  $\text{CuIn}_{1-x}\text{Ga}_x\text{Se}_2$  thin films with different Ga ratios and (b) for  $\text{CuIn}_{0.9}\text{Ga}_{0.1}\text{Se}_2$  films with different thicknesses (color online)

Data of the extinction coefficient  $k$  shown in Fig. 12 reveal that, it decreases with increasing  $\lambda$  in the visible spectral range, then it increases with  $\lambda$  in the NIR region ( $\lambda$

$> 1000$  nm). This may be attributed to the characteristic feature of existence of free carriers [40, 44].

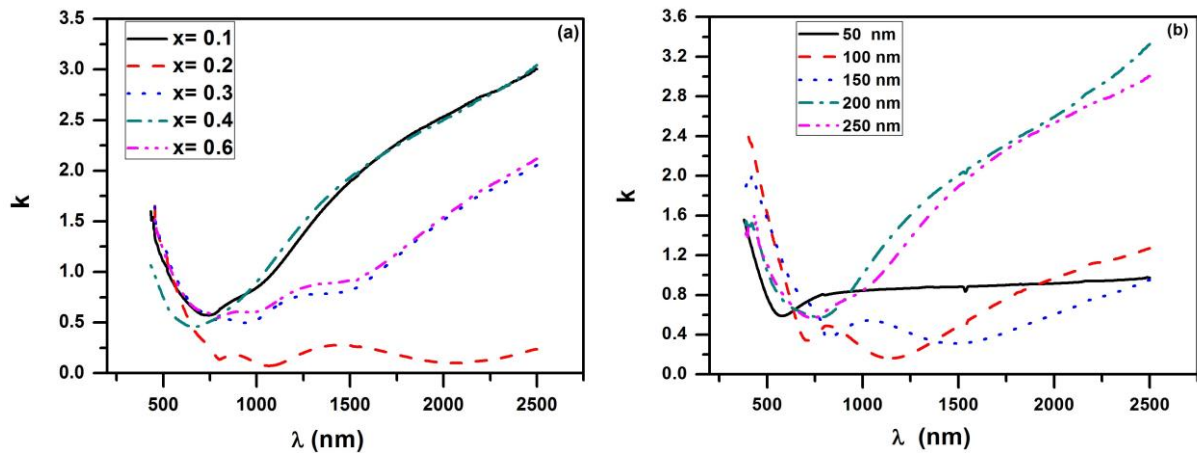


Fig. 12. (a) The extinction coefficient  $k$  versus  $\lambda$  for as – deposited  $\text{CuIn}_{1-x}\text{Ga}_x\text{Se}_2$  thin films with different Ga ratios and (b) for different thicknesses  $\text{CuIn}_{0.9}\text{Ga}_{0.1}\text{Se}_2$  thin films (color online)

Fig. (13 a, b & c) reveals the effect of annealing process at 573 K for different time periods (5 – 60 min.) on  $\alpha$ ,  $n$  and  $k$  of  $\text{CuIn}_{0.9}\text{Ga}_{0.1}\text{Se}_2$  thin films of 250 nm thick, respectively. It can be concluded that, the annealing process, in general, inhibits these parameters over the whole considered  $\lambda$ - range, excluding over the range  $\sim 670$ - 830 nm of  $\lambda$ , they are relatively enhanced. This behavior could be correlated to the films microstructure changes by annealing and the conditions of their

preparation. Besides, the calculated values for  $n$  are around 2.5 for all annealed films almost over the whole considered range ( $\sim 500$ -2500nm) of  $\lambda$ . They are more reasonable than  $\sim 8 - 30$  values of the pre- annealed film (Fig. 13 b) and are comparable to the values ranging from 2.61- 2.72 calculated for CIGS over the range 1700-2200 nm of  $\lambda$  [46] and the value of 2.9 reported for both  $\text{CuInSe}_2$  and  $\text{CuGaSe}_2$  single crystals [1,45].

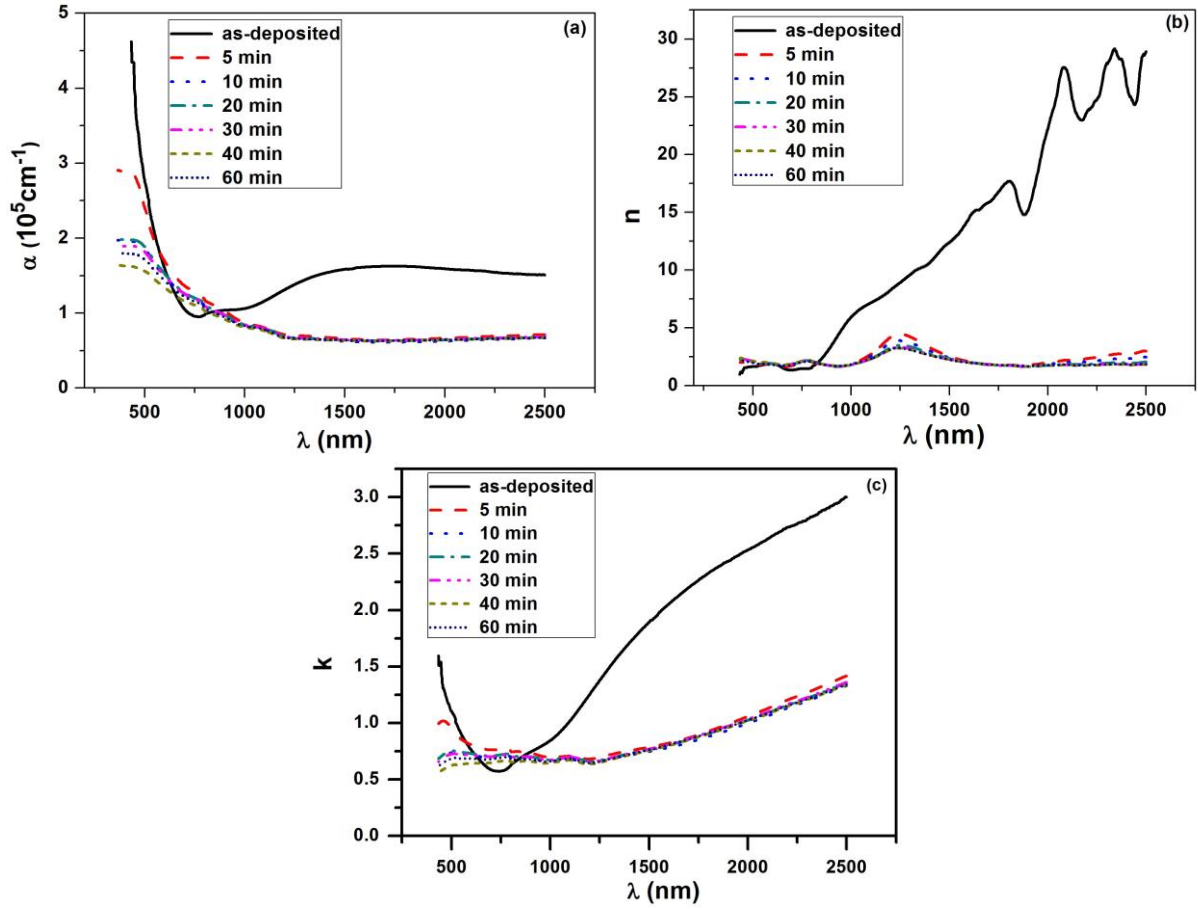


Fig. 13. (a, b and c): variations of  $\alpha$ ,  $n$  and  $k$  versus  $\lambda$ , respectively for as - deposited and annealed at 573 K for different periods of time  $\text{CuIn}_{1-x}\text{Ga}_x\text{Se}_2$  thin films (color online)

At high enough absorption levels ( $\alpha > 10^4 \text{ Cm}^{-1}$ ) in semiconducting glasses, the absorption coefficient  $\alpha$  obey the following spectral equation [6, 46]:

$$\alpha h\nu = B (h\nu - E_g)^r \quad (8)$$

where  $B$  is a temperature independent constant that depends on the effective mass and the refractive index and  $E_g$  is the optical band gap. In agreement with many other works [6, 25, 42] the absorption coefficient  $\alpha$  calculated for the present CIGS films seemed to obey the direct allowed transition relation, for which the exponent  $r = 1/2$ .

Fig. 14 gives  $(\alpha h\nu)^2$  vs.  $h\nu$  dependence for as - deposited  $\text{Cu In}_{1-x}\text{Ga}_x\text{Se}_2$  thin films of 250 nm thick with different compositions, as an example. The intercept of the linear portions with  $(\alpha h\nu)^2 = 0$  has been utilized to deduce the energy gap value. Variations of the calculated  $E_g$  values with Ga - ratio in CIGS films having different thicknesses are depicted in Fig. 15. It is shown that,  $E_g$ , in general, decreases as the film thickness increases, which might be due to the probable increase of the disorder in the microstructure of the relatively thicker films, causing the band tails in the forbidden band to increase.

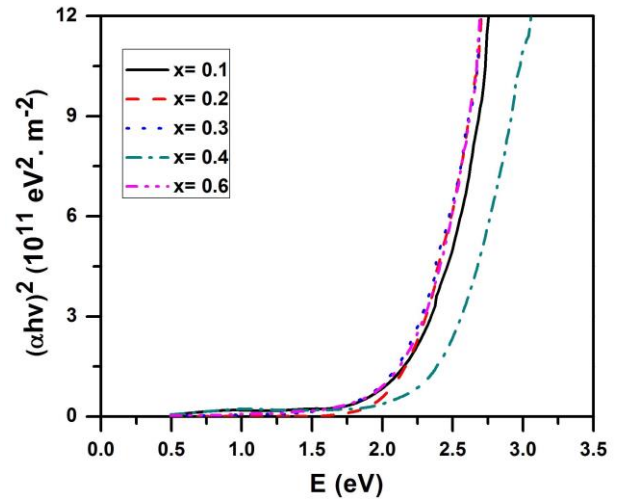


Fig. 14.  $(\alpha h\nu)^2$  vs.  $h\nu$  dependence for as - deposited  $\text{Cu In}_{1-x}\text{Ga}_x\text{Se}_2$  films of 250 nm thick with different compositions (color online)

The CIGS films having different thicknesses are depicted in Fig. 15. It is shown that,  $E_g$ , in general, decreases as the film thickness increases, which might be due to the probable increase of the disorder in the microstructure of the relatively thicker films, causing the band tails in the forbidden band to increase. Besides, the

observed decrease of  $E_g$  values for films as Ga –ratio increases up to  $x = 0.3$  followed by its increase for the relatively Ga - rich films ( $x > 0.3$ ) could be attributed to the change in crystallinity degree of film microstructure revealed by XRD (Fig. 1b).

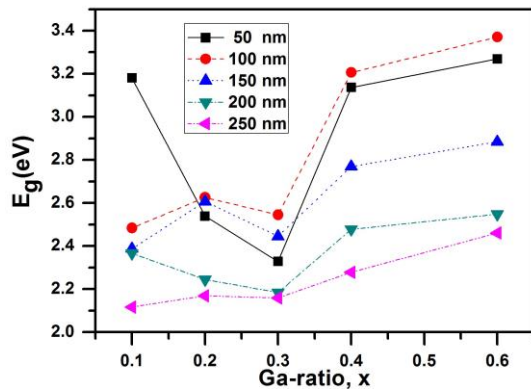


Fig. 15. The dependence of the optical band gap  $E_g$  on the Ga ratio for as - deposited  $\text{CuIn}_{1-x}\text{Ga}_x\text{Se}_2$  thin films with different thicknesses (color online)

The influence of heat treatment at 573 K for time periods elongation from 5 to 60 min. on  $E_g$  values of CIGS films of  $\sim 250$  nm thick is shown in Fig. (16). The observed enhancement of  $E_g$  values caused by annealing may be consistent with the fact that, the heat treatment changes the amount of disorder and the number of defects present in the amorphous structure leading to the crystallinity increase, which has been proven by XRD examination; ( See Fig. (2)).

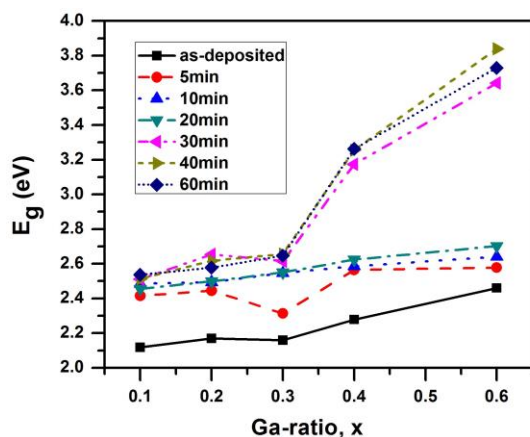


Fig. 16. The dependence of the optical band gap  $E_g$  with Ga ratio for as - deposited and annealed at 573 K for different periods of time  $\text{CuIn}_{1-x}\text{Ga}_x\text{Se}_2$  250 nm thick (color online)

Furthermore, minimum values of  $E_g$  have been obtained when the Ga –ratio was 0.3 for either as – deposited or annealed films (Fig. 15&16). This ratio (0.3) of Ga– ratio is considered by many works [22, 24&34] to be the optimal  $[\text{Ga}] / [\text{In} + \text{Ga}]$  ratio of CIGS solar cell absorber layer. These minimum values of  $E_g$  are in the range  $\sim 2.55 - 2.12$  eV for the as – deposited films as

their thicknesses increase from 100 nm to 250 nm, and in the range  $\sim 2.33 - 2.64$  eV after film annealing at 573 K with elongation of the time periods from 5 – 60 min. respectively. These  $E_g$  values, which are higher than its favorable (1.04 - 1.68 eV) values [22, 24&34] could improve the open circuit voltage  $V_{OC}$  [2, 22-24].

#### 4. Conclusions

CIGS thin films of 50 – 250 nm thick and Ga – ratio of 0.1 up to 0.6 have been synthesized by thermal deposition technique from its initial bulk form prepared by usual melt quench method. The effects of Ga – ratio, film thickness and annealing at 573 K for periods extended to 60 min. on the film structure, surface morphology, composition stoichiometry as well as the optical properties has been investigated. Different structural and optical parameters were determined and discussed.

Polycrystalline bulk  $\text{CuIn}_{1-x}\text{Ga}_x\text{Se}_2$  structure with a little distortion due to the formed tiny secondary phases has been obtained. CIGS films are chalcopyrite with (112) preferred orientation either before or after annealing process. The revealed amorphous matrix by XRD and SEM suggest the partially amorphous structure of the present as – deposited and annealed CIGS thin films. Non – uniform and less dense surface of films, even after annealing at 573 K for 60 min. could be observed. Besides, some deviation in film stoichiometric composition was also depicted.

However, the present relatively thinner films have proved to possess high absorption coefficient ( $10^5 \text{ cm}^{-1}$ ), refractive index ( $\sim 2.5$ ) close to the reported 2.61 – 2.72 values and the value of 2.9 for both  $\text{CuInSe}_2$  and  $\text{CuGaSe}_2$  single crystals [1, 45] and direct energy gap. Besides, the present CIGS film with Ga-ratio of 0.3 has higher absorption coefficient ( $\alpha > 10^5 \text{ cm}^{-1}$ ) and smaller energy gap value (2.12 – 2.64 eV) among other films, coinciding with the optimal Ga –ratio for the highest efficiency of cells.

The present insufficient results for high efficient CIGS thin film absorber layer may be due to the decreased crystallinity in a film and / or the inconvenient preferred orientation (112 or 204/220) of crystalline growth that significantly effect on the physical properties of a material [35]. It is believed that, an accurate control of the composition constituent elements as well as a further heat treatment may be demanded for more improvement of the parameters of crystalline growth of these partially amorphous films and in turn their physical properties could be improved.

#### References

- [1] Y. Yan, S. Li, Y. Ou, Y. Ji, C. Yan, L. Liu, Z. Yu, Y. Zhao, J. Mod. Transport **22**(1), 37 (2014).
- [2] J. Liu, D. Zhuang, M. Cao, X. Li, M. Xie, D. Xu, J. Vacuum, School of Materials Science and Engineering **102**, 26 (2014)

- [3] A. Chirila, S. Buecheler, F. Pianezzi, P. Bloesch, C. Gretener, A. R. Uhl, C. Fella, L. Kranz, J. Perrenoud, S. Seyrling, R. Verma, S. Nishiwaki, Y. E. Romanyuk, G. Bilger, A. N. Tiwari, *Nat. Mater.* **10**, 857 (2011).
- [4] M. A. Contreras, B. Egaas, K. Ramanathan, J. Hiltner, A. Swartzlander, F. Hasoon, R. Noufi, *Progr. Photovoltaics Res. Appl.* **7**, 311 (1999).
- [5] E. Wallin, U. Malm, T. Jarmar, O. Lundberg, M. Edoff, L. Stolt, *Progr. Photovoltaics Res. Appl.* **20**, 851 (2012).
- [6] J. Athar, *Turk J. Phys.* **31**, 287 (2007).
- [7] T. Tanaka, Y. Demizu, A. Yoshida, *J. Appl. Phys.* **81**, 7619 (1997).
- [8] D. Haneman, *Crit. Rev. Solid State Mater. Sci.* **14**, 377 (1988).
- [9] N. Abdullah Al-Hamadani, F. Ibrahim Mustafa, J. Jasim Al-Kabi, *J. Advancement in Engineering Technology, Management and Appli. Sci. (IJAETMAS)*, 05(2017) 24-33.
- [10] M. Lammer, U. Klemm, M. Powalla, *Thin Solid Films* **387**(1), 33 (2001).
- [11] A. Amara, A. Ferdi, A. Drici, J. C. Bernède, M. Morsli, M. Guerioune, *Catal Today* **113**(3), 251 (2006).
- [12] J. A. Frantz, R. Y. Bekele, V. Q. Nguyen, J. S. Sanghera, A. Bruce, S. V. Frolov, I. D. Aggarwal, *Thin Solid Films* **519**(22), 7763 (2011).
- [13] D. Y. Lee, S. Park, J. H. Kim, *Current Applied Physics* **11**(1), 88 (2011).
- [14] S. N. Alamri, H. F. Alsadi, *J. of Korean Physical Society* **67**(2), 350 (2015).
- [15] J. Liu, D. Zhuang, H. Luan, M. Cao, M. Xie, X. Li, *Progress in natural Science: Materials International* **23**(2), 133 (2013).
- [16] M. Kaelin, D. Rudmann, A. N. Tiwari, *Solar Energy* **77**, 749 (2004).
- [17] K. Kushiya, *Solar Energy Materials and Solar Cells* **93**, 1037 (2009).
- [18] S. Zulfiqar, E. Yassitepe, M. Ilyas Sarwar, S. Ismat Shah, *J. Mater Sci: Mater. Electron.* **24**, 3226 (2013).
- [19] P. Jackson, D. Hariskos, E. Lotter, S. Paetel, R. Wuerz, R. Menner, W. Wischmann, M. Powalla, *Progr. Photovoltaics Res. Appl.* **7**, 894 (2011).
- [20] P. Jackson, R. Wuerz, D. Hariskos, E. Lotter, W. Witte, M. Powalla, *Phys. Status Solidi, Rapid Res. Letters* **10**, 583 (2016).
- [21] Takuya Kato, *Jap. J. Appl. Phys.* **56**(04), CA02 (2017).
- [22] C. L. Jensen, D. E. Tarrant, J. H. Ermer, G. A. Pollock. In: Conference record of the twenty Third IEEE photovoltaic specialists conference, Louisville, Kentucky, 577 (1993).
- [23] J. R. Tuttle, M. Contreras, A. Tennant, D. Albin, R. Noufi, In: photovoltaic specialists conference, 1993, Conference record of the Twenty Third IEEE, Louisville, Kentucky, 415 (1993).
- [24] U. Rau, H. W. Schock, *Cu(In, Ga) Se<sub>2</sub> thin-film solar cells: materials, manufacture and operation.* Oxford: Elsevier, 303 (2005).
- [25] Nabeel A. Bakr, Nidhal N. Jandow, Nadir F. Habubi, *International letters of Chemistry Physics and Astronomy* **39**, 52 (2014).
- [26] A. A. Akl, S. A. Aly, H. Howari, *Chalcogen. Lett.* **13**(6), 247 (2016).
- [27] H. P. Klug, L. E. Alexander, *X-Ray Diffraction Procedures*, Wiley, New York, 1954.
- [28] Y. Liu, D. Kong, J. Li, C. Zhao, C. Chen, *Science Direct* **16**, 217 (2012).
- [29] E. P. Zaretskya, V. F. Gremenok, V. F. Riede, W. Schmitz, K. Bente, V. B. Zalesski, O. V. Ermakov, *J. Phys. and Chem. of Solids* **64**, 1989 (2003).
- [30] A. Kropidowska, J. Chojnacki, A. Fahmi, B. Becker, *Dalton Trans.* **47**, 6825 (2008).
- [31] V. Bilgin, S. Kose, F. Atay, I. Akyuz, *Mater. Chem. Phys.* **94**, 103 (2005).
- [32] Z. R. Khan, M. Zulfequar, Mohd. Shahid Khan, *Mater. Sci. Eng. B* **174**, 145 (2010).
- [33] Yuz, Yan Y. Lis et al., *Appl. Surf. Sci.* **264**, 197 (2013).
- [34] J. R. Tuttle, M. Conteras, A. Tennant, D. Albin, R. Noufi, *Proceeding of the 23<sup>rd</sup> IEEE, photovoltaic specialists conference*, 415 (1993).
- [35] M. A. Contreras, M. J. Romero, R. Noufi, *J. Thin solid films* **511-512**, 51 (2006).
- [36] P. Jackson, R. Wurz, U. Rau et al., *Progress in Photovoltaics* **6**(15), 507 (2007).
- [37] T. S. Moss, *Optical Properties of Semiconductors*, Academic Press, New York, 40 (1959).
- [38] E. Kh. Shokr., *J. Phys. and Chem. of Solids* **53**, 1215 (1992).
- [39] F. Yakuphanoglu, M. Sekerci, O. F. Ozturk, *Optics Communications* **239**, 275 (2004).
- [40] A. A. M. Farag, M. Abdel Rafea, N. Roushdy, O. El-Shazly, E. F. El-Wahidy, *J. Alloys and Compounds* **621**, 434 (2015).
- [41] H. M. Zeyada, M. M. El-Nahass, S. A. Samak, *J. Non-Cryst. Solids* **358**, 915 (2012).
- [42] A. Ashery, A. A. M. Farag, M. A. Shenashen, *Synthetic Metals* **162**, 1357 (2012).
- [43] H. Neumann, W. Horig, E. Recciu, H. Sobotta, B. Schumann, G. Kuhn, *Thin Solid Films* **61**, 13 (1979).
- [44] H. M. Zeyada, M. M. El-Nahass, I. S. Elashmaui, A. A. Habashi, *J. Non-cryst. solids* **358**, 625 (2012).
- [45] K. C. Park, D. Y. Ma, K. H. Kim, *Thin Solid Films* **305**, 201 (1997).
- [46] N. F. Mott, E. A. Davis, *Electronic process in Non crystalline Materials*, (Clarendon Press, Oxford, 1979).

---

\*Corresponding author: mostafa.wakkad@yahoo.com,  
m.wakkad@science.sohag.edu.eg